JOURNAL OF CHEMICAL & ENGINEERING DATA

ARTICLE

pubs.acs.org/jced

Complexation of 1,3-Bis(tris(hydroxymethyl)methylamino)propane Systems Involving Divalent (Cobalt, Nickel, or Zinc) Ions in Aqueous Solution by Potentiometry

Thomas Laureys,[†,‡] Isabel S. S. Pinto,[†] Claúdia V. M. Soares,[†,§] Hari B. Boppudi,[†] and Helena M. V. M. Soares*[,†]

[†]REQUIMTE, Departamento de Engenharia Química, Faculdade de Engenharia, Universidade do Porto, 4200-465, Porto, Portugal

[‡]Department of Biochemistry and Microbiology, KaHo St.-Lieven, Industrial Engineering, Gebroeders Desmetstraat 1, B-9000 Gent, Belgium

[§]Engenharia e Sistemas, EFACEC, Apartado 3003, Rua Eng. Frederico Ulrich, 4471-907 Moreira da Maia, Portugal

ABSTRACT: Protonation constants of 1,3-bis(tris(hydroxymethyl)methylamino)propane (BTP) and the complexes formed between BTP and Co(II), Ni(II), or Zn(II) metal ions have been studied by glass electrode potentiometry (GEP) in aqueous 0.1 mol·L^{-1} KNO_3 supporting electrolyte at 25 ± 0.1 °C. The complexation model for each M(II)−BTP system was established. The proposed final model for Ni(II)−BTP system is: NiL, $NiLH_{-1}$, and $NiLH_{-2}$, with stability constant values, as log β, of 7.13 ± 0.02, −1.32 ± 0.04, and −10.81 ± 0.05, respectively. For Co(II)−BTP and Zn(II)−BTP systems, the proposed final model is constituted by ML, ML_2, ML_2H_{-1}, and ML_2H_{-2} complexes. For the Co(II)−BTP system, the overall refined stability constants (as log β) are 4.57 ± 0.02, 8.76 ± 0.02, 0.17 ± 0.03, and −8.73 ± 0.03, respectively, and for Zn(II)−BTP system they are 4.99 ± 0.02, 9.18 ± 0.03, 1.01 ± 0.03, and −7.91 ± 0.04, respectively. In a general way, the complex stability was found to follow the trend: Ni(II) > Zn(II) > Co(II).

1. INTRODUCTION

Hydrogen buffers are used to maintain a constant concentration of hydrogen ions in solution. The hydrogen donor/acceptor can be oxygen, as is the case of phosphate; however, for many biological buffers nitrogen acts as a donor/acceptor since a variety of substituents can tailor the amine pK_a to neutral pH. Due to this, the choice of alternative buffers had greatly increased with the commercial availability of the zwitterionic *N*-substituted aminosulfonic acids synthesized by Good and co-workers.[1−3] Good's buffers have, in fact, been widely adopted, and at least one major chemical supplier devotes a special section of its catalog to them (e.g., Sigma-Aldrich).

The compound 1,3-bis(tris(hydroxymethyl)methylamino)propane (BTP) is commercially available from Sigma-Aldrich. Its pH buffering ranges between 6.3 and 9.5, which comprises a large pH range and makes it suitable for a wide broader of applications. To exemplify this statement, the literature describes many works where BTP has been used as a buffer for multipurposes.[4−8]

Studies involving metal ions (such as is the case of heavy metals speciation, biological, and biochemical studies), which require pH control, are inevitably subject to the possibility of buffer interference as a result of metal complexation. So, when these buffers are used in studies involving metal ions in solution, it is very important to consider the possible interference of them, due to metal ion complexation. If complexes are formed, then stability constants must be known.

From the analysis of the structure of the BTP (Figure 1), we see that BTP contains two secondary amines plus six hydroxyl groups on the β carbons. From this, we can clearly anticipate that BTP should be a strong complexing agent. Previous works, where the interactions between BTP and Cu(II)[9] or Ni(II)[10] were studied, evidenced that BTP forms strong complexes with these two metal ions in the pH buffer range and thus can decrease strongly the free metal ion concentration when this ligand is used as a buffer. However, the reported values of the protonation constants and the complex-forming features of BTP with Ni(II)[9,10] were determined without the reference of a set of a minimum criteria.[11,12] In this context, the protonation constants of BTP and the equilibrium solution studies of the interaction between this ligand and Ni(II) were revisited and reevaluated in the present work. Additionally, the formation constants of the complexes in aqueous solution with BTP and the Co(II) and Zn(II) metal ions were also determined in this work for the first time.

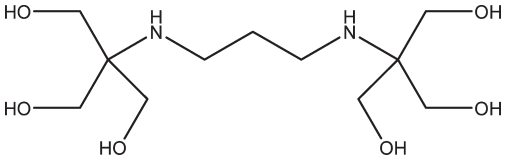

Figure 1. Structure of 1,3-bis(tris(hydroxymethyl)methylamino)propane (BTP).

2. EXPERIMENTAL SECTION

2.1. Materials and Methods. The ligand BTP (99 %) was purchased from Sigma-Aldrich (St. Louis, Missouri, USA) and used as received. Solutions of Co(II) and Ni(II) were prepared

Received: July 28, 2011
Accepted: September 29, 2011
Published: October 27, 2011

ACS Publications © 2011 American Chemical Society

Table 1. Experimental Conditions Used in the Determination of Global Protonation Constants of BTP and of Global Stability Constants in M(II)−BTP Systems, by GEP, at 25° C and μ = 0.1 mol·L^{-1} (KNO_3)

		$[L_T]$	$[M_T]$	
ligand or metal	$[L_T]$:$[M_T]$	mol·L^{-1}	mol·L^{-1}	pH range
BTP		$1.0\cdot10^{-3}$		3.4−11.9
		$2.5\cdot10^{-3}$		3.4−11.9
Co(II)	2		$1.0\cdot10^{-3}$	3.2−10.1
	3		$4.0\cdot10^{-3}$	3.8−11.0
	4		$1.0\cdot10^{-3}$	2.8−11.7
Ni(II)	2		$1.0\cdot10^{-3}$	3.3−11.6
	4		$1.0\cdot10^{-3}$	3.0−11.7
Zn(II)	4		$1.0\cdot10^{-3}$	2.7−12.0
	6		$1.0\cdot10^{-3}$	3.9−11.3

from Merck analytical grade of $Ni(NO_3)_2$ and $Co(NO_3)_2$ and standardized by ethylenediaminetetraacetate (EDTA) complexometric titrations.[13] An acidic standard solution of Zn(II) ($1.5\cdot10^{-2}$ mol·L^{-1}) purchased from Merck was used. Additional information about the remaining reagents is described elsewhere.[14]

2.2. Potentiometric Measurements. The potentiometric titrations of BTP and of M(II)−BTP systems [M = Co(II), Ni(II), or Zn(II)] were performed using an automatic acquisition data with a personal computer (PC) controlled system, as previously described.[14] All measurements were performed on solutions adjusted to an ionic strength of 0.1 M with KNO_3 in a Methrom (Herisau, Switzerland) jacketed glass vessel, equipped with a magnetic stirrer, and thermostatted at 25.0 ± 0.1 °C using a water bath. A stream of purified nitrogen was used as the inert atmosphere in the titration cells to degas all solutions before the titrations. Oxygen and carbon dioxide were excluded from the reaction mixture by maintaining a slight positive pressure of purified nitrogen in the titration cell.

The glass electrode calibration, in terms of hydrogen ion concentration, was accomplished by the addition of a standardized solution of potassium hydroxide to a standardized solution of nitric acid (both solutions adjusted to the ionic strength of 0.1 mol·L^{-1}). From this potentiometric titration, the values of $E°$ and response slope were obtained by fitting a straight line to the experimental points collected around pH 2 and 11.

The protonation constants of BTP, as well as the metal stability constants of BTP with Co(II), Ni(II), and Zn(II) metal ions, were all determined by direct potentiometric titrations using glass electrode potentiometry (GEP). For all systems, monotonic titrant volume additions of standardized KOH were made, and the potential was recorded as a function of the added volume. For the determination of protonation constants of BTP, three solutions with a BTP concentration of $2.5\cdot10^{-3}$ mol·L^{-1} and other three solutions with a concentration of $1.0\cdot10^{-3}$ mol·L^{-1} were used; for each solution, two titrations were performed. Further experimental details are described in Table 1.

For all M(II)−BTP systems studied, pH-potentiometric titrations were performed using the fixed total ligand-to-total-metal-ion concentration ($[L_T]$:$[M_T]$) ratios over a wide pH range. For the Co(II)−BTP system, a total of nine titrations were carried out; for the refining operations of the stability constants, five titrations from four independent solutions with the $[L_T]$:$[M_T]$ ratio set to 4, $[Co^{2+}] = 1.0\cdot10^{-3}$ mol·L^{-1}, and two titrations from a different solution with the $[L_T]$:$[M_T]$ ratio at 3, $[Co^{2+}] = 4.0\cdot10^{-3}$ mol·L^{-1} were used. Additionally, two more titrations from another solution with $[L_T]$:$[M_T]$ ratio set to 2, $[Co^{2+}] = 1.0\cdot10^{-3}$ mol·L^{-1}, were also performed. For the Ni(II)−BTP system, five independent solutions were prepared, and a total of eight titrations was performed using $[L_T]$:$[M_T]$ ratios of 2 and 4, $[Ni^{2+}] = 1.0\cdot10^{-3}$ mol·L^{-1}. In the case of the Zn(II)−BTP system, five independent solutions were prepared to perform seven titrations. A total of five titrations were carried out with the $[L_T]$:$[M_T]$ ratio set to 4, and the other two were at a $[L_T]$:$[M_T]$ ratio of 6; in all titrations, the concentration of Zn(II) was $1.0\cdot10^{-3}$ mol·L^{-1}.

The $[L_T]$:$[M_T]$ ratios used to characterize M(II)−BTP systems, as well as other experimental details, are compiled in Table 1.

2.3. Data Treatment. For the refinement of the protonation constants of BTP, the water constant[15] (Table 2) was kept constant. During the refinement of the overall metal stability constants for all systems, the water and BTP protonation constants, as well as all known stability constants for $M_x(OH)_y$ species[15] (Table 2), were kept fixed.

The simulation and optimization procedures of potentiometric data was done using the ESTA (equilibrium simulation for titration analysis) program.[16,17] The refinement operation involves solving mass-balance equations, including the equation for the total proton concentration, in such a way that the computed free proton concentration, when used by the equation describing the response of the calibrated glass electrode, reproduces the experimentally recorded potential of the glass electrode as accurately as possible. This is done by minimization of an objective function, U, defined as:

$$U = (N - n_p)^{-1} \sum_{n=1}^{N} (E_n^{obs} - E_n^{calc})^2 \quad (1)$$

where U is the objective function to be minimized, N is the total number of experimental titration points, n_p represents the number of parameters simultaneously optimized, E_n^{obs} is observed electrode potential at the nth data point and $E_n^{calc} = E^0 + k \log[H^+]$, E^0 is the electrode intercept, and k is the electrode calibration slope. The Gauss−Newton method is the adopted approach by ESTA to minimize U.

The Hamilton R-factor, R^H, is the statistical parameter used by ESTA to reflect the improved agreement between calculated and observed data. It is given by:

$$R^H = \left[\frac{U}{\sum_{n=1}^{N} (E_n^{obs})^2} \right]^{1/2} \quad (2)$$

ESTA software includes a metal formation function, Z_M, defined by:[18]

$$Z_M = \frac{L_T - L(1 + \sum_{n=1}^{N} \beta_{n01}[H^+]^n)}{M_T} \quad (3)$$

where

$$L = \frac{H_T - [H^+] + [OH^-]}{\sum_{n=1}^{N} \beta_{n01}[H^+]^n} \quad (4)$$

dx.doi.org/10.1021/je200809m |J. Chem. Eng. Data 2012, 57, 87–92

Table 2. Protonation Constants for Water, BTP, and Overall Stability Constants for M(II) Complexes with OH^-, at 25.0 °C

	equilibrium	log β	μ / mol·L^{-1}	reference
water	$H^+ + OH^- \leftrightarrow H_2O$	13.78	0.1	15
BTP	$L^{2-} + H^+ \leftrightarrow HL^-$	9.07 ± 0.01	0.1	this work[a]
	$L^{2-} + 2H^+ \leftrightarrow H_2L$	15.95 ± 0.01	0.1	
Co(II)	$Co^{2+} + H_2O \leftrightarrow [Co(OH)]^+ + H^+$	−9.5	0.0	15
	$Co^{2+} + 2H_2O \leftrightarrow [Co(OH)_2] + 2H^+$	−18.4	0.0	15
	$Co^{2+} + 3H_2O \leftrightarrow [Co(OH)_3]^- + 3H^+$	−30.8	0.0	15
	$Co(OH)_2(s) \leftrightarrow Co^{2+} + 2OH^-$	−14.9	0.0	15
Ni(II)	$Ni^{2+} + H_2O \leftrightarrow [Ni(OH)]^+ + H^+$	−10.2	0.1	15
	$Ni^{2+} + 2H_2O \leftrightarrow [Ni(OH)_2] + 2H^+$	−18.6	0.0	15
	$Ni^{2+} + 3H_2O \leftrightarrow [Ni(OH)_3]^- + 3H^+$	−29.3	0.0	15
	$Ni(OH)_2$ (s) $\leftrightarrow Ni^{2+} + 2OH^-$	−15.1	0.0	15
Zn(II)	$Zn^{2+} + H_2O \leftrightarrow [Zn(OH)]^+ + H^+$	−9.2	0.1	15
	$Zn^{2+} + 2H_2O \leftrightarrow [Zn(OH)_2] + 2H^+$	−16.5	0.0	15
	$Zn^{2+} + 3H_2O \leftrightarrow [Zn(OH)_3]^- + 3H^+$	−27.7	0.0	15
	$Zn(OH)_2$ (s) $\leftrightarrow Zn^{2+} + 2OH^-$	−15.52	0.1	15

[a] For this refinement, a total of 831 points were used in a pH range between 3.4 and 11.9.

L_T, M_T, and H_T represent the total concentration of ligand, metal, and proton, respectively; β_{n01} stands for the formation constants of the $M_nL_0H_l$ species. This function is calculated for each datum point and is plotted against −log[L] to aid in the modeling procedures. Model selection was mainly based on the following criteria:[19] (i) a search for the minimum value of the objective function being minimized; (ii) good internal consistency of the data; (iii) best fit between experimental and calculated formation curves for the different models tested; and (iv) calculations of the degree of formation of each species using species distribution diagrams (SDD).

3. RESULTS AND DISCUSSION

3.1. Protonation Constants of BTP. The protonation constants obtained after the refinement of the results using all titrations performed with BTP concentrations of ($1.0 \cdot 10^{-3}$ and $2.5 \cdot 10^{-3}$) mol·L^{-1} (Table 1) were, for log β_1 and β_2, 9.07 ± 0.01 and 15.95 ± 0.01, respectively (Table 2).

A comparison of the values of the protonation constants observed with BTP and propylenediamine (PPDM) (log K_1 = 10.54 and log K_2 = 6.31)[15] and 1,3-diamino-2-propanol (log K_1 = 9.56 and log K_2 = 8.02)[15] evidence that, for K_1, the acidic character of these compounds follow the trend: BTP > 1,3-diamino-2-propanol > PPDM. This behavior is explicable as the presence of hydroxyl groups in the neighborhood of the amine groups of 1,3-diamino-2-propanol and BTP decreases the electron density of the amines and thus increases their acidity.

3.2. Models and Complexation Stability Constants of the Co(II)−BTP System. For the Co(II)−BTP system, complexation studies were performed with a $1 \cdot 10^{-3}$ mol·L^{-1} metal concentration for [L_T]:[Co_T] ratios of 2 and 4 and a $4.0 \cdot 10^{-3}$ mol·L^{-1} metal concentration for a [L_T]:[Co_T] ratio of 3. Two models, model I [CoL, $CoLH_{-1}$, and $CoLH_{-2}$] and model II [CoL, CoL_2, CoL_2H_{-1}, and CoL_2H_{-2}], were used to refine the Co(II)−BTP system. For [L_T]:[Co_T] ratios 3 and 4, both models were tested, and equivalent results were obtained for both [L_T]:[Co_T] ratios; for [L_T]:[Co_T] ratio 4, refinement operations are presented in Table 3. The analysis of the results shows that the stability constant values obtained for the CoL species, by the two models, are equivalent. Besides CoL, we also included $CoLH_{-1}$ and $CoLH_{-2}$ in model I and CoL_2, CoL_2H_{-1}, and CoL_2H_{-2} in model II. For the two individual [L_T]:[Co_T] ratios studied, the ESTA program was able to refine both models well. However, the fitting for model I [CoL + $CoLH_{-1}$ + $CoLH_{-2}$] did not improve the results, and a worse Hamilton *R*-factor was obtained than for model II. On the other hand, if one considers that $CoLH_{-1}$ and $CoLH_{-2}$ are formed from the hydrolysis of the CoL complex, the refined stability constants for both species have unrealistic values. A comparison between log β for $CoLH_{-1}$ (−3.03) and $CoLH_{-2}$ (−12.00) with the theoretical ones [$\log_{10} \beta$ $CoLH_{-1}$ = $\log_{10} \beta$ CoL + $\log_{10} \beta$ Co(OH) = 4.65 + (−9.5) = −4.85 and $\log_{10} \beta$ $CoLH_{-2}$ = $\log_{10} \beta$ CoL + $\log_{10} \beta$ $Co(OH)_2$ = 4.65 + (−18.4) = −13.75] shows that the first ones are significantly larger than the computed values of −4.85 and −13.75. Such a huge increase (about 1.8 log units above the theoretical values) would mean that the formation of $CoLH_{-1}$ and $CoLH_{-2}$ involved a major structural change of the complexes, which is most unlikely. When we analyze the Z_M of model II for a [L_T]:[Co_T] ratio of 4 (Figure 2A), it is clear that the Z_M function increases above 1 and goes straight up to 2. So, CoL_2 could be the species necessary to complete the model.[18] After 2, the Z_M graphic starts curving. This means that there is formation of the $CoL_x(H_{-1})_y$ species.[18] Besides this, the Z_M graphical analysis (Figure 2A) shows that model II, the model constituted by CoL, CoL_2, CoL_2H_{-1}, and CoL_2H_{-2} species, reproduced perfectly the experimental results in the pH range considered (model II, Table 3). In addition, the log β values for CoL_2H_{-1} (−0.17) and CoL_2H_{-2} (−9.29) are closer to the theoretical ones [CoL_2H_{-1} = CoL_2 + Co(OH) = 8.67 + (−9.5) = −0.83; CoL_2H_{-2} = CoL_2 + $Co(OH)_2$ = 8.67 + (−18.4) = −9.73], which is additional evidence of model II.

To test the proposed model, a species distribution diagram (SDD) was generated for [L_T]:[Co_T] ratios of 2 and 4 (Figure 3). Figure 3A does not predict precipitation at the [L_T]:[Co_T] ratio of 4, which is in agreement with the experimental work. This figure also suggests that CoL, CoL_2, and CoL_2H_{-2} are the major

dx.doi.org/10.1021/je200809m |J. Chem. Eng. Data 2012, 57, 87–92

Table 3. Overall Stability Constants (as $\log_{10}\beta$ Values) for One Titration for the M(II)−BTP Systems Determined by GEP in 0.1 mol·L^{-1} KNO_3 at 25 °C; for All M(II)−BTP Systems, [M(II)] = 1·10^{-3} mol·L^{-1}

metal	Co(II)		Ni(II)		Zn(II)	
$[L]:[M]_T$	4		4		6	
equilibrium	model I	model II	model I	model II	model I	model II
$M^{2+} + L^{2-} \leftrightarrow ML$	4.648 ± 0.009	4.610 ± 0.006	7.25 ± 0.01	7.24 ± 0.01	4.73 ± 0.02	4.74 ± 0.01
$M^{2+} + 2L^{2-} \leftrightarrow ML_2$	NI[a]	8.667 ± 0.006	NI	10.12 ± 0.01	NI	8.88 ± 0.01
$M^{2+} + L^{2-} + H_2O \leftrightarrow MLH_{-1} + H^+$	−3.03 ± 0.01	NI	−1.41 ± 0.01	NI	−2.85 ± 0.01	NI
$M^{2+} + L^{2-} + 2H_2O \leftrightarrow MLH_{-2} + 2H^+$	−12.00 ± 0.02	NI	−11.89 ± 0.02	NI	−10.55 ± 0.02	NI
$M^{2+} + 2L^{2-} + H_2O \leftrightarrow ML_2H_{-1} + H^+$	NI	−0.17 ± 0.01	NI	1.28 ± 0.01	NI	0.90 ± 0.01
$M^{2+} + 2L^{2-} + 2H_2O \leftrightarrow ML_2H_{-2} + 2H^+$	NI	−9.29 ± 0.01	NI	−9.41 ± 0.02	NI	−7.75 ± 0.01
Hamilton *R*-factor	0.01	0.006	0.005	0.003	0.016	0.008
number of points	96	96	103	103	132	132
pH range	6.0−9.0	6.0−9.0	5.5−10.0	5.5−10.0	5.9−8.5	5.9−8.5

[a] NI: not included.

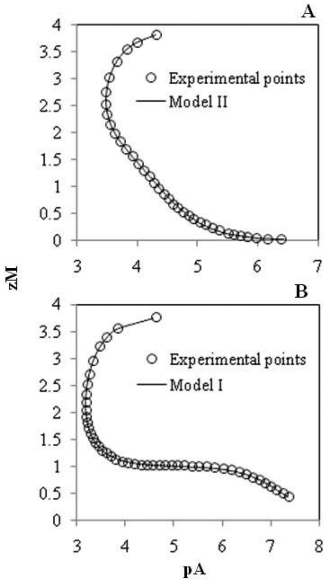

Figure 2. Z_M function for (A) Co(II)−BTP and (B) Ni(II)−BTP systems. Models and experimental conditions are described in Table 3.

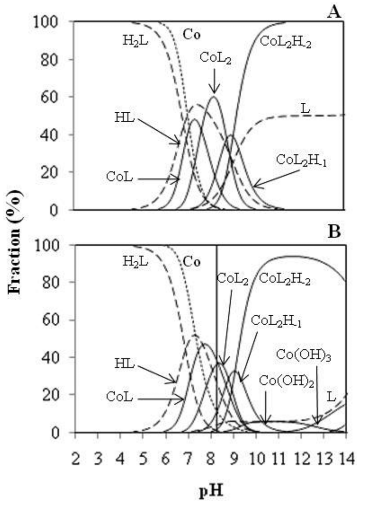

Figure 3. Species distribution diagrams computed for the Co(II)−BTP system using model II of Table 3. (A) $[L_T]:[Co_T]$ = 4, $[Co_T]$ = 1.0·10^{-3} mol·L^{-1}. (B) $[L_T]:[Co_T]$ = 2, $[Co_T]$ = 1.0·10^{-3} mol·L^{-1}. The vertical line indicates $Co(OH)_2$ precipitation (full line).

species, and for this model the best statistical result was obtained (Table 3). Figure 3B predicts, at the $[L_T]:[Co_T]$ ratio of 2, mainly the formation of CoL and CoL_2 prior the precipitation to occur at about pH 8. At this $[L_T]:[Co_T]$ ratio, the GEP experiment confirmed that it was impossible to collect data in the whole pH range due to occurrence of precipitation. Thus, the proposed final model should include CoL, CoL_2, CoL_2H_{-1}, and CoL_2H_{-2} species. The final overall stability constants resulting from the simultaneous refinement in ESTA of all titrations performed for $[L_T]:[Co_T]$ ratios of 3 and 4 are presented in Table 4.

3.3. Models and Complexation Stability Constants of the Ni(II)−BTP System. For refining operations of the Ni(II)−BTP system, two models were assumed, model I [NiL, $NiLH_{-1}$, and $NiLH_{-2}$] and model II [NiL, NiL_2, NiL_2H_{-1}, and NiL_2H_{-2}], and two different $[L_T]:[Ni_T]$ ratios ($[L_T]:[Ni_T]$ ratios 2 and 4, $[Ni^{2+}]$ = 1.0·10^{-3} mol·L^{-1}) were used to establish the correct model. Final results obtained, after refining both models of one titration for the $[L_T]:[M_T]$ ratio of 4, are summarized in Table 3.

Table 3 shows that the fitting of the two models (I and II) generated almost equivalent statistical parameters of the overall fitting, indicating that both models can probably represent the system at this ratio. From the analysis of the Z_M function (Figure 2B), it is noticed that Z_M increases straight up to 1. This means that NiL is formed. Figure 2B also shows that the formation of NiL occurs in a wide range of pH, as the Z_M remains constant at 1, in a pA range between 6.2 to 4, which corresponds to a pH range between 6.1 to 7.

On the other hand, the presence of NiL_2 in model II, as a major metal containing species is not supported by the graphical analysis of Z_M function since after Z_M attains a value of 1, the graphic does not go straight up to 2 but it immediately starts to curve; these facts clearly suggest the formation of $NiL(H_{-1})_y$ and/or $Ni(OH)_z$ species.[18] In addition, the refined value for

dx.doi.org/10.1021/je200809m |J. Chem. Eng. Data 2012, 57, 87–92

Table 4. Overall Stability Constants (as $\log_{10}\beta$ Values), Refined Simultaneously for All Titrations in ESTA, for BTP with Co(II), Ni(II), and Zn(II) in 0.1 mol·L^{-1} KNO_3 at 25 °C

equilibrium	log β
$Co^{2+} + L^{2-} \leftrightarrow CoL$	4.57 ± 0.02
$Co^{2+} + 2L^{2-} \leftrightarrow CoL_2^{2-}$	8.76 ± 0.02
$Co^{2+} + 2L^{2-} + H_2O \leftrightarrow CoL_2H_{-1} + H^+$	0.17 ± 0.03
$Co^{2+} + 2L^{2-} + 2H_2O \leftrightarrow CoL_2H_{-2} + 2H^+$	−8.73 ± 0.03
no. points	907
no. titrations/no. independent solutions	7/5
$Ni^{2+} + L^{2-} \leftrightarrow NiL$	7.13 ± 0.02
$Ni^{2+} + L^{2-} + H_2O \leftrightarrow NiLH_{-1} + H^+$	−1.32 ± 0.04
$Ni^{2+} + L^{2-} + 2H_2O \leftrightarrow NiLH_{-2} + 2H^+$	−10.81 ± 0.05
no. points	720
no. titrations/no. independent solutions	8/5
$Zn^{2+} + L^{2-} \leftrightarrow ZnL$	4.99 ± 0.02
$Zn^{2+} + 2L^{2-} \leftrightarrow ZnL_2^{2-}$	9.18 ± 0.03
$Zn^{2+} + 2L^{2-} + H_2O \leftrightarrow ZnL_2H_{-1} + H^+$	1.01 ± 0.03
$Zn^{2+} + 2L^{2-} + 2H_2O \leftrightarrow ZnL_2H_{-2} + 2H^+$	−7.91 ± 0.04
no. points	646
no. titrations/no. independent solutions	7/5

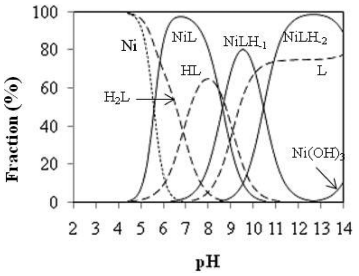

Figure 4. Species distribution diagram computed for the Ni(II)−BTP system using model I of Table 3. $[L_T]:[Ni_T]$ = 4, $[Ni_T]$ = $1.0 \cdot 10^{-3}$ mol·L^{-1}.

NiL_2 (10.12) does not present a realistic value as it is much lower than two times the value of the refined value for NiL.

After this modeling exercise, we concluded that the proposed final model for the Ni(II)−BTP system is: NiL, $NiLH_{-1}$, and $NiLH_{-2}$. To confirm the proposed model, SDD was drawn for the experimental conditions studied (Figure 4). SDD indicates that NiL, $NiLH_{-1}$, and $NiLH_{-2}$ are predominant species in the pH range where they are formed; this behavior was observed no matter what $[L_T]:[Ni_T]$ ratio was used. In the case of NiL species, SDD evidenced that this species is formed at a large extent (more than 90 %) in a wide pH range (about two pH units), which is consistent with the presence of a plot of NiL, as it is shown by the graphical analysis of Z_M function (Figure 2B).

The final overall stability constants resulting from the simultaneous refinement operations of all $[L_T]:[Ni_T]$ ratios are presented in Table 4.

The comparison of the value of the NiL stability constant observed with BTP (7.13) (Table 4) and propylenediamine (PPDM) (6.31)[15] shows that Ni(II) binds more strongly with BTP. A simple evaluation based on the basicity of the two ligands points out to enlargement in the stability constant values with the increase of the pK_a,[11] which was not observed. The fact that NiL stability constant is

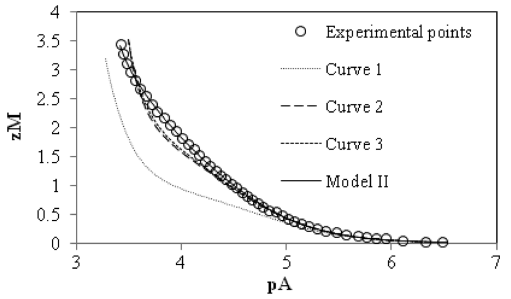

Figure 5. Z_M function for the Zn(II)−BTP system. Theoretical models (curves 1 to 3) are calculated from ZnL_x constants in Table 3 and Zn−$(OH)_y$ constants in Table 2 (for further details see text). The refined model (model II) and experimental conditions are described in Table 3.

0.8 log units higher than for Ni−PPDM system, though the basicity of BTP is smaller than for PPDM, suggests that BTP's hydroxyl(s) groups are involved in the coordination.

3.4. Models and Complexation Stability Constants of the Zn(II)−BTP System. To characterize the Zn(II)−BTP system and to establish the correct model, two different $[L_T]:[Zn_T]$ ratios were studied by GEP (Table 1). In the case of the Zn(II)−BTP system, a similar refinement was also accomplished, as it was done for the other two M(II)−BTP systems. Model I [ZnL + $ZnLH_{-1}$ + $ZnLH_{-2}$] and model II [ZnL + ZnL_2 + ZnL_2H_{-1} + ZnL_2H_{-2}] were fitted without a problem. The final results are summarized in Table 3.

The fitting of the two models (I and II) generated almost equivalent statistical parameters of the overall fitting (Table 3), which indicates that both models can probably represent the system. In the case of the $[L_T]:[Zn_T]$ ratio equal to 6, the experimental Z_M function (Figure 5) shows that the Z_M function grows almost linearly until 2 without back fanning;[18] this behavior suggests the formation of ZnL and ZnL_2.

For both models, the same value of ZnL was refined (Table 3). This indicates that ZnL should be a major species. From ESTA refinement, the log β_{ZnL_2} value was 8.88. If the value of the stability constant for ZnL is about 4.74, then the expected log β_{ZnL_2} value should be about 9.5 (twice the log K_{ZnL}) or a little bit lower; the refined value, 8.88, from model II (Table 3) is in agreement with this statement.

For model I, the values obtained for the stability constants for the hydroxide species, $ZnL(H_{-1})_y$, are a bit larger than the expected ones. For $ZnLH_{-1}$, the theoretical value would be −4.47 [$\log \beta_{ZnLH_{-1}} = \log \beta_{ZnL} + \log \beta_{Zn(OH)} \leftrightarrow \log \beta_{ZnLH_{-1}} = 4.73 + (-9.2)$] and for $ZnLH_{-2}$ −11.8 [$\log \beta_{ZnLH_{-2}} = \log \beta_{ZnL} + \log \beta_{Zn(OH)_2} \leftrightarrow \log \beta_{ZnLH_{-2}} = 4.73 + (-16.5)$], while the ones obtained experimentally are larger (model I, Table 3). Using the same procedure, the theoretical values for $ZnL_2(H_{-1})_y$ complexes are: $\log \beta_{ZnL_2H_{-1}} = \log \beta_{ZnL_2} + \log \beta_{Zn(OH)} \leftrightarrow \log \beta_{ZnL_2H_{-1}} = 8.88 + (-9.2) = -0.32$, $\log \beta_{ZnL_2H_{-2}} = \log \beta_{ZnL_2} + \log \beta_{Zn(OH)_2} \leftrightarrow \log \beta_{ZnL_2H_{-2}} = 8.88 + (-16.5) = -7.62$; in the case of the ZnL_2H_{-2} complex, the refined stability constant value, $\log \beta_{ZnL_2H_{-2}} = -7.75 \pm 0.01$ (Table 3), is of similar magnitude to the one predicted theoretically.

Using these theoretical values, three Z_M were generated (Figure 5, curves 1 to 3). Analysis of Z_M for models described by curves 1 [with $ZnL(H_{-1})_y$ species fixed at theoretical values] and 2 [with $ZnL_2(H_{-1})_y$ species fixed at theoretical values] in Figure 5 suggests that $ZnL_2(H_{-1})_y$ species are major species at higher pH values (pA lower than 4); curve 2 is much closer to experimental

dx.doi.org/10.1021/je200809m |J. Chem. Eng. Data 2012, 57, 87–92

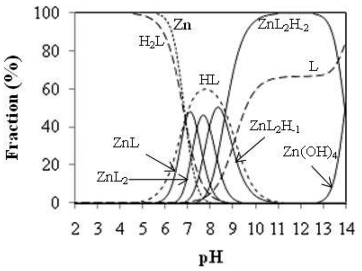

Figure 6. Species distribution diagrams computed for the Zn(II)−BTP system using model II of Table 3. $[L_T]:[Zn_T]$ = 6, $[Zn_T]$ = $1.0 \cdot 10^{-3}$ mol·L^{-1}.

Z_M than curve 1, which means that $ZnL(H_{-1})_y$ species exist in a small amount. This is also confirmed when curves 2 and 3 are compared; including all of the $ZnL_x(H_{-1})_y$ species, fixed at theoretical values (curve 3, Figure 5), the difference between curves 2 and 3 is minimal, evidencing that the contribution of $ZnL(H_{-1})_y$ species is small. Taking into account all of these facts, the solid line (model II) represents the major species present in solution, with refined stability constant values indicated in Table 3. From a statistical point of view, no more species are required to reproduce the objective function. To obtain additional evidence of the model, tentative attempts to determine the stability constants for zinc and BTP by differential pulse polarography at a $[L_T]:[Zn_T]$ = 101, $[Zn^{2+}]$ = $1 \cdot 10^{-5}$ mol·L^{-1} in the pH range 4 and 11 were performed; however, after the addition of the ligand, BTP, to the zinc ion in solution, the system became irreversible, which disabled the determination.

To test the proposed model, a SDD was generated for the experimental $[L_T]:[Zn_T]$ conditions used ($[L_T]:[Zn_T]$ = 6, $[Zn^{2+}]$ = $1 \cdot 10^{-3}$ mol·L^{-1}) assuming model II as the correct one (Figure 6). The SDD evidence that ZnL and ZnL_2 are major species but are formed in a narrow pH range. On the other hand, SDD shows that ZnL_2H_{-1} starts to be formed immediately after the ZnL_2 is being formed, and this is probably the explanation why an equivocally linear increase of Z_M up to 2 was not attained (Figure 5).

All of the facts described above strongly suggest that model II is the correct one. Considering all of the $[L_T]:[Zn_T]$ ratios for which the final model [ZnL, ZnL_2, ZnL_2H_{-1}, and ZnL_2H_{-2}] was refined, the final overall stability constant values were obtained and are presented in Table 4.

AUTHOR INFORMATION

Corresponding Author

*E-mail: hsoares@fe.up.pt. Mailing address: Helena Soares, Departamento de Engenharia Química, Faculdade de Engenharia do Porto, Rua Dr. Roberto Frias, 4200-465, Porto, Portugal. Phone number: +351-225081650; fax number: +351-225081449.

Funding Sources

One of us (H.B.B.) acknowledges a grant scholarship (SFRH/BPD/43913/2008) financed by the "Fundação para a Ciência e a Tecnologia" (FCT) from the Portuguese Government. We also thank Professor Carlos Gomes from the Faculty of Sciences/Porto University for the COPOTISY program.

REFERENCES

(1) Good, N. E.; Winget, G. D.; Winter, W.; Connolly, T. N.; Izawa, S.; Singh, R. M. M. Hydrogen ion buffers for biological research. *Biochemistry* **1966**, *5*, 467–477.

(2) Good, N. E.; Izawa, S. Hydrogen ion buffers. *Methods Enzymol.* **1972**, *24*, 53–68.

(3) Ferguson, W. J.; Braunschweiger, K. I.; Braunschweiger, W. R.; Smith, J. R.; McCormick, J. J.; Wasmann, C. C.; Jarvis, N. P.; Bell, D. H.; Good, N. E. Hydrogen-ion buffers for biological-research. *Anal. Biochem.* **1980**, *104*, 300–310.

(4) Sadecka, J.; Polonsky, J. Determination of organic acids in tobacco by capillary isotachophoresis. *J. Chromatogr., A* **2003**, *998*, 161–165.

(5) Meissner, T.; Einsenbeiss, F.; Jastorff, B. Determination of anionic trace impurities in glycerol by capillary isotachophoresis with enlarged sample load. *J. Chromatogr., A* **1998**, *810*, 201–208.

(6) Doble, P.; Andersson, P.; Haddad, P. R. Determination and prediction of transfer ratios for anions in capillary zone electrophoresis with indirect UV detection. *J. Chromatogr., A* **1997**, *770*, 291–300.

(7) Keller, C. P.; Van Volkenburgh, E. Osmoregulation by oat coleoptile protoplasts—Effect of auxin. *Plant Physiol.* **1996**, *110*, 1007–1016.

(8) Hunt, B. E.; Mandoli, D. F. Axenic cultures of acetabularia (chlorophyta)—A decontamination protocol with potential application to other algae. *J. Physiol.* **1992**, *28*, 407–414.

(9) Hong, K. H.; Bai, K. S. Copper(II) complexation by 2-((3-((2-hydroxy-1,1-di(hydroxymethyl)ethyl)amino)propyl)amino)-2-(hydroxymethyl)-1,3-propanediol in aqueous solution. *Bull. Korean Chem. Soc.* **1998**, *19*, 197–201.

(10) Bai, K. S.; Hong, K. H. Formation of nickel(II) complexes of 1,3-bis(tris(hydroxymethyl)methylamino)propane in aqueous solution. *Bull. Korean Chem. Soc.* **2000**, *21*, 650–652.

(11) Martell, A. E.; Hancock, R. D. *Metal Complexes in Aqueous Solutions*; Plenum Press: New York, 1996.

(12) Filella, M.; May, P. M. Reflections on the calculation and publication of potentiometrically-determined formation constants. *Talanta* **2005**, *65*, 1221–1225.

(13) Flaschks, H. A. *EDTA Titrations*; Pergamon Press: New York, 1959.

(14) Machado, C. M. M.; Cukrowski, I.; Gameiro, P.; Soares, H. M. V. M. Challenges in modelling and optimization of stability constants in the study of metal complexes with monoprotonated ligands Part I: A glass electrode potentiometric and polarographic study of a Cu-TAPSO-OH system. *Anal. Chim. Acta* **2003**, No. 493, 105–119.

(15) Martell, A. E.; Smith, R. M. *NIST Standard Reference Database 46 Version 8.0, NIST Critically Selected Stability Constants of Metal Complexes Database*; U.S. Department of Commerce, National Institute of Standards and Technology: Gaithersburg, MD, 2004.

(16) May, P. M.; Murray, K.; Williams, D. R. The use of glass electrodes for the determination of formation constants - II. Simulation of titration data. *Talanta* **1985**, *32*, 483–489.

(17) May, P. M.; Murray, K.; Williams, D. R. The use of glass electrodes for the determination of formation constants - III. Optimization of titration data - the ESTA library of computer programs. *Talanta* **1988**, *35*, 825–830.

(18) Marsicano, F.; Monberg, C.; Martincigh, B. S.; Murray, K.; May, P. M.; Williams, D. R. The existence and stability of mixed-ligand complexes in aqueous solutions containing zinc and cyanide ions at elevated pH values. *J. Coord. Chem.* **1988**, *16*, 321–339.

(19) Bugarin, M. G.; Filella, M. The formation constants of dimethylthallium(III)-glutathione complexes in aqueous solution. *J. Inorg. Biochem.* **1999**, *73*, 17–29.